

Black Hole Outflows

A. R. King¹

¹*Theoretical Astrophysics Group, University of Leicester, Leicester LE1 7RH*

4 September 2018

ABSTRACT

I show that Eddington accretion episodes in AGN are likely to produce winds with velocities $v \sim 0.1c$ and ionization parameters up to $\xi \sim 10^4$ (cgs), implying the presence of resonance lines of helium- and hydrogenlike iron. These properties are direct consequences of momentum and mass conservation respectively, and agree with recent X-ray observations of fast outflows from AGN. Because the wind is significantly sub-luminal, it can persist long after the AGN is observed to have become sub-Eddington. The wind creates a strong cooling shock as it interacts with the interstellar medium of the host galaxy, and this cooling region may be observable in an inverse Compton continuum and lower-excitation emission lines associated with lower velocities. The shell of matter swept up by the (‘momentum-driven’) shocked wind must propagate beyond the black hole’s sphere of influence on a timescale $\lesssim 3 \times 10^5$ yr. Outside this radius the shell stalls unless the black hole mass has reached the value M_σ implied by the $M - \sigma$ relation. If the wind shock did not cool, as suggested here, the resulting (‘energy-driven’) outflow would imply a far smaller SMBH mass than actually observed. In galaxies with large bulges the black hole may grow somewhat beyond this value, suggesting that the observed $M - \sigma$ relation may curve upwards at large M . Minor accretion events with small gas fractions can produce galaxy-wide outflows with velocities significantly exceeding σ , including fossil outflows in galaxies where there is little current AGN activity. Some rare cases may reveal the energy-driven outflows which sweep gas out of the galaxy and establish the black hole–bulge mass relation. However these require the quasar to be at the Eddington luminosity.

Key words: accretion: accretion discs – galaxies: formation – galaxies: active – black hole physics

1 INTRODUCTION

Outflows and winds are widely observed in many types of galaxies, from active to normal (e.g. Chartas et al., 2003; Pounds et al., 2003a, 2006; O’Brien et al., 2005, Holt et al., 2008; Krongold et al., 2007; Tremonti et al., 2007). There is often a strong presumption that the central supermassive black hole (SMBH) is implicated. Although other types of driving exist, e.g. by supernovae or starbursts, in many cases these phenomena are themselves associated with accretion episodes on to the SMBH.

From a theoretical viewpoint, outflows driven by black holes offer a simple way of establishing relations between the SMBH and its host galaxy, and hence potential explanations for the $M - \sigma$ and $M - M_{\text{bulge}}$ relations (Ferrarese & Merritt, 2000; Gebhardt et al. 2000; Häring & Rix 2004). Such outflows are plausible, as AGN must feed at high rates to grow the observed SMBH masses, given the short duty cycle implied by the rarity of AGN among all galaxies. There is

no obvious reason why these rates should respect the hole’s Eddington limit, and outflows are a natural consequence.

However it is unclear just how, if at all, the various types of observed outflows mentioned in the first paragraph fit together in terms of these ideas. This paper aims to clarify this.

2 THE EDDINGTON RATIO IN AGN

Super-Eddington accretion is widely observed in accreting binary systems. For example the well-known system SS433 has an Eddington ratio $\dot{m} = \dot{M}/\dot{M}_{\text{Edd}}$ of order 5000 (e.g. King et al., 2000; Begelman et al., 2006). Here \dot{M} , \dot{M}_{Edd} are the accretion rate and the Eddington value respectively.

The distinctive feature of AGN accretion is that such large Eddington ratios are unlikely. To see this we note that the maximum possible accretion rate is the dynamical rate

$$\dot{M}_{\text{dyn}} \simeq \frac{f_g \sigma^3}{2G}, \quad (1)$$

The dynamical rate applies when a gas mass which was previously self-supporting against gravity is destabilized and falls freely on to the black hole. Equation (1) describes the case where gas is initially in rough virial equilibrium in the bulge of a galaxy with velocity dispersion σ and baryonic mass fraction f_g . Parametrizing, we find

$$\dot{M}_{\text{dyn}} \simeq 1.4 \times 10^2 \sigma_{200}^3 M_{\odot} \text{ yr}^{-1} \quad (2)$$

where $\sigma_{200} = \sigma/(200 \text{ km s}^{-1})$, and we have taken $f_g = 0.16$. We compare this with

$$\dot{M}_{\text{Edd}} = \frac{L_{\text{Edd}}}{\eta c^2} = \frac{4\pi GM}{\kappa \eta c} \quad (3)$$

where L_{Edd} is the Eddington luminosity, η the radiative efficiency of accretion, and κ the electron scattering opacity. We evaluate this for $\eta = 0.1$ and black hole masses M lying close to the observed $M - \sigma$ relation

$$M \simeq 2 \times 10^8 M_{\odot} \sigma_{200}^4 \quad (4)$$

to find

$$\dot{M}_{\text{Edd}} \simeq 4.4 \sigma_{200}^4 M_{\odot} \text{ yr}^{-1} \quad (5)$$

and thus an Eddington ratio

$$\dot{m} < \frac{\dot{M}_{\text{dyn}}}{\dot{M}_{\text{Edd}}} \simeq \frac{33}{\sigma_{200}} \simeq \frac{39}{M_8^{1/4}} \quad (6)$$

where $M_8 = M/10^8 M_{\odot}$. Since $0.1 \lesssim M_8 \lesssim 10$ for the black holes in AGN, and \dot{M}_{dyn} is an upper limit to \dot{M} , modest values $\dot{m} \sim 1$ of the Eddington ratio are likely.

For completeness I note that much higher Eddington ratios can occur if the gas mass which is destabilized was previously held together by self-gravity, e.g. as in a star. In this case we find a maximum dynamical rate $\dot{M}_{\text{dyn}} \sim v_{\text{orb}}^3/2G \sim M_*/P$, where M_* is the stellar mass and v_{orb}, P its orbital velocity and period. This gives rates $\dot{M}_{\text{dyn}} \sim 0.1 M_{\odot}/\text{hr}$ in stellar-mass binary systems. Rather lower values result for tidal disruption of stars near SMBH because the stellar debris is only accreted over a spread in orbital times (e.g. Lodato et al., 2009).

3 SMBH WINDS AT MODEST EDDINGTON RATIOS

Motivated by the results of the previous section, I examine the properties of winds from SMBH accreting with modest Eddington ratios $\dot{m} \sim 1$. I assume that the winds are quasi-spherical, over solid angle $4\pi b$, with $b \sim 1$ (this is confirmed for PG1211+143; Pounds & Reeves, 2009). It is well known that winds of this type have electron scattering optical depth $\tau \sim 1$ measured from infinity in to a distance of order the Schwarzschild radius $R_s = 2GM/c^2$ (e.g. King & Pounds, 2003). This means that on average every emitted photon scatters about once before escaping to infinity, which in turn suggests that the total wind momentum must be of order the photon momentum, i.e.

$$\dot{M}_{\text{out}} v \simeq \frac{L_{\text{Edd}}}{c}, \quad (7)$$

as is for example also found for the winds of hot stars. Using (3) gives the wind velocity

$$v \simeq \frac{\eta}{\dot{m}} c \sim 0.1c. \quad (8)$$

This agrees with the fact that winds are always found to have a terminal velocity typical of the escape velocity from the radius at which they are launched, here several tens of R_s . As expected, using this value of v in the mass conservation equation

$$\dot{M}_{\text{out}} = 4\pi b R^2 v \rho(R), \quad (9)$$

where $\rho(R)$ is the mass density, self-consistently shows that the optical depth τ of the wind is ~ 1 (cf King & Pounds, 2003, eqn. 4).

Since the wind moves with speed $\sim 0.1c$, it can persist long after the AGN is observed to have become sub-Eddington. The duration of the lag is $\sim 10R/c$, where R is the radial extent of the wind (i.e. the shock radius, as we shall see below). For $R \gtrsim 3$ pc this lag is at least a century, and far longer lags are possible, as we shall see. This may be the reason why AGN showing other signs of super-Eddington phenomena (e.g. narrow-line Seyfert 2 galaxies) are nevertheless seen to have sub-Eddington luminosities (e.g. NGC 4051: Denney et al., 2009).

We can use (8, 9) to estimate the ionization parameter

$$\xi = \frac{L_i}{NR^2} \quad (10)$$

of the wind. Here $L_i = l_i L_{\text{Edd}}$ is the ionizing luminosity, with $l_i < 1$ a dimensionless parameter specified by the quasar spectrum, and $N = \rho/\mu m_p$ is the number density. This gives

$$\xi = 3 \times 10^4 \eta_{0.1}^2 l_2 \dot{m}^{-2}, \quad (11)$$

where $l_2 = l_i/10^{-2}$, and $\eta_{0.1} = \eta/0.1$.

Equation (11) shows that the wind momentum and mass rates determine its ionization parameter: for a given quasar spectrum, the predominant ionization state is such that the threshold photon energy defining L_i , and the corresponding ionization parameter ξ , together satisfy (11). This requires high excitation: a low threshold photon energy (say in the infrared) would imply a large value of l_2 , but the high value of ξ then given by (11) would require the presence of very highly ionized species, physically incompatible with such low excitation.

For suitably chosen continuum spectra, it is possible to envisage a range of solutions of (11), and it is even possible that a given spectrum may allow more than one solution, the result being specified by initial conditions. However for a typical quasar spectrum, an obvious self-consistent solution of (11) is $l_2 \simeq 1$, $\dot{m} \simeq 1$, $\xi \simeq 3 \times 10^4$. This describes the case where the quasar is currently radiating at the Eddington limit. However as remarked after eqn (9), we can also have situations where the quasar's luminosity has dropped after an Eddington episode, but the wind is still flowing, with $\dot{m} \simeq 1$. In this case the ionizing luminosity $10^{-2} l_2 L_{\text{Edd}}$ in (11) takes a lower value, giving a lower value of ξ . For example a quasar of luminosity $0.3 L_{\text{Edd}}$ would have $\xi \sim 10^4$. This corresponds to a photon energy threshold appropriate for helium- or hydrogenlike iron (i.e. $h\nu_{\text{threshold}} \sim 9 \text{ keV}$).

We conclude that

Eddington winds from AGN are likely to have velocities $\sim 0.1c$, and show the presence of helium- or hydrogenlike iron.

A number of such winds are known (see Cappi, 2006, for a review). This Section shows that it is no coincidence that in

all cases the wind velocity is $v \sim 0.1c$, and further that they are all found by identifying blueshifted resonance lines of Fe XXV, XXVI in absorption. Conversely, any observed wind with these properties automatically satisfies the momentum and mass relations (7, 9), strongly suggesting launching by an AGN accreting at a slightly super-Eddington rate.

Two further remarks are relevant here. We note first that (7) implies a kinetic energy rate

$$\frac{1}{2}\dot{M}_{\text{out}}v^2 \simeq \frac{v}{c}L_{\text{Edd}} \simeq \frac{\eta}{2}L_{\text{Edd}} \simeq 0.05L_{\text{Edd}} \quad (12)$$

implying a mechanical ‘energy efficiency’ $\eta/2 \simeq 0.05$ wrt L_{Edd} . Cosmological simulations typically adopt such values in order to produce an $M - \sigma$ relation in agreement with observation (e.g. di Matteo, 2005). As we have seen, this implicitly means that they adopt the single-scattering momentum relation (7). We shall see below (in Section 5) that there must also be an implicit assumption of momentum rather than energy driving, i.e. that the wind interacts with the host galaxy through its ram pressure rather than its energy.

I note that the near-Eddington regime considered here differs from the hyper-Eddington regime discussed by Shakura & Sunyaev (1973), where the much larger optical depth leads to the energy relation $\dot{M}_{\text{out}}v^2/2 \simeq L_{\text{Edd}}$ instead of the momentum relation (7). This generally only holds in accreting stellar-mass binary systems (see Section 6 below), but King (2009) discusses a possible case involving super-massive black holes.

Finally, we should also note that although we assume here that Eddington or super-Eddington accretion leads to winds and outflow, some authors have considered alternative possibilities. The main observational constraint on these ideas is the Soltan argument (Soltan, 1982). This relates the background radiation of the Universe to the mass density in supermassive black holes, and with subsequent work (e.g. Yu & Tremaine, 2002) is generally interpreted as implying that most of the mass of the SMBH in galaxy centres results from luminous accretion with a typical radiative efficiency $\eta \sim 0.1$.

However since the value of η appearing in the Soltan argument is a global average over many different accretion events, it is clearly still possible for some fraction of the mass growth to occur in other ways which produce little outflow, as for example in the so-called Polish doughnuts (see Abramowicz, 2009, for a recent review). This type of accretion flow could reduce or even remove the mechanical feedback between black hole growth and the host galaxy. The fact that the $M - \sigma$ relation emerges (without free parameter) from consideration of momentum-driven Eddington winds tends to support the straightforward interpretation of the Soltan argument adopted here, but one should be alive to alternative possibilities.

4 INTERACTION WITH THE HOST

It is clear that an Eddington wind of the type discussed above can have a significant effect on its host galaxy. The kinetic power of the wind is

$$\dot{M}_{\text{out}} \frac{v^2}{2} = \frac{v}{2c}L_{\text{Edd}} \simeq 0.05L_{\text{Edd}} \quad (13)$$

where we have used (7) and (8). If the wind persists as the hole doubles its mass (i.e. for a Salpeter time), its total energy is $\simeq 5 \times 10^{59} M_8$ erg, where M_8 is the hole mass in units of $10^8 M_\odot$. This formally exceeds the binding energy $\sim M_{\text{bulge}}\sigma^2 \sim 3 \times 10^{58}$ erg of a galaxy bulge with baryonic mass $M_{\text{bulge}} \sim 10^{11} M_\odot$ and velocity dispersion $\sigma \sim 200 \text{ km s}^{-1}$ (as suggested by the $M - M_{\text{bulge}}$ and $M - \sigma$ relations). Evidently the coupling of wind energy to the galaxy must be inefficient, as black holes would destroy or at least severely modify their host bulges in any significant super-Eddington growth phase.

To investigate this we must consider how the wind interacts with the interstellar medium of the host. Just as in the corresponding problem for a stellar wind, the interaction must successively involve an inner (reverse) shock, slowing the central wind, a contact discontinuity between the shocked wind and the shocked, swept-up interstellar medium, and an outer (forward) shock driven into this medium and sweeping it outwards, ahead of the shocked wind (see Fig. 1). The inefficient coupling of wind energy to the galactic baryons noted above strongly suggests that the shocked wind cools rapidly after passing through the inner shock. This removes the thermal pressure generated in the shock, and leaves only the preshock ram pressure acting on the interstellar medium. A clear candidate for this shock cooling is the inverse Compton effect on the quasar’s radiation field (King, 2003). We note that this typically has Compton temperature $T_c \sim 10^7$ K, whereas the formal temperature at the inner adiabatic shock is $m_p v^2/k \sim 10^{11}$ K. The quasar radiation cools the inner shock efficiently, provided that this is within galaxy-scale distances from the centre (King, 2003). Inverse Compton cooling should produce a component in the quasar spectrum characterized by $kT_c \sim 1$ keV and with a luminosity $\sim \dot{M}_{\text{out}}v^2/2 \simeq 0.05L_{\text{Edd}}$, i.e. about 5% of the quasar’s bolometric output. I note that even if the quasar becomes sub-Eddington, leaving a wind persisting for a lag time $10R_{\text{shock}}/c$, its radiation field is still able to cool the shock efficiently.

Given this efficient cooling, the inner (adiabatic) shock and very narrow associated cooling region together constitute an ‘isothermal shock’. The gas density jumps by a factor ~ 4 at the adiabatic shock, accompanied by a velocity drop by the same factor. It is then strongly compressed in the cooling region while the velocity slows to low values (see Fig. 2). Since the cooling is efficient the whole region is very thin compared with the shock radius R_{shock} , and we can regard the shock as locally plane. The Rankine-Hugoniot relations across this isothermal shock then show that the mass flow rate ρv remains constant, while the postshock gas pressure drops to the value

$$P_{\text{ram}} = \rho v^2 = \frac{\dot{M}v}{4\pi b R_{\text{shock}}^2} \simeq \frac{L_{\text{Edd}}}{4\pi b R_{\text{shock}}^2 c}, \quad (14)$$

i.e. the preshock ram pressure. With a constant cooling time, as expected, the postshock temperature and velocity u drop approximately linearly with distance behind the shock, and the density rises as $1/u$, strongly increasing its emission measure. The gas is likely to be in photoionization equilibrium as it has low optical depth to the quasar radiation, and the increased densities imply short recombination times. The mass conservation equation (9) and ionization parameter (10) combine to give

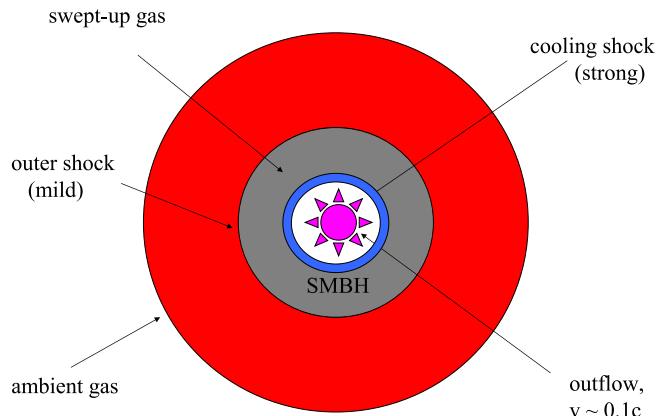


Figure 1. Schematic view of the shock pattern resulting from the impact of an Eddington wind on the interstellar gas of the host galaxy. A supermassive black hole (SMBH) accreting at just above the Eddington rate drives a fast wind (velocity $u = v \sim \eta c \sim 0.1c$), whose ionization state makes it observable in X-ray absorption lines. The outflow collides with the ambient gas in the host galaxy and is slowed in a strong shock. The inverse Compton effect from the quasar’s radiation field rapidly cools the shocked gas, removing its thermal energy and strongly compressing and slowing it over a very short radial extent. This gas may be observable in an inverse Compton continuum and lower-excitation emission lines associated with lower velocities. The cooled gas exerts the preshock ram pressure on the galaxy’s interstellar gas and sweeps it up into a thick shell (‘snowplough’). This shell’s motion drives a milder outward shock into the ambient interstellar medium. This shock ultimately stalls unless the SMBH mass has reached the value M_σ satisfying the $M - \sigma$ relation.

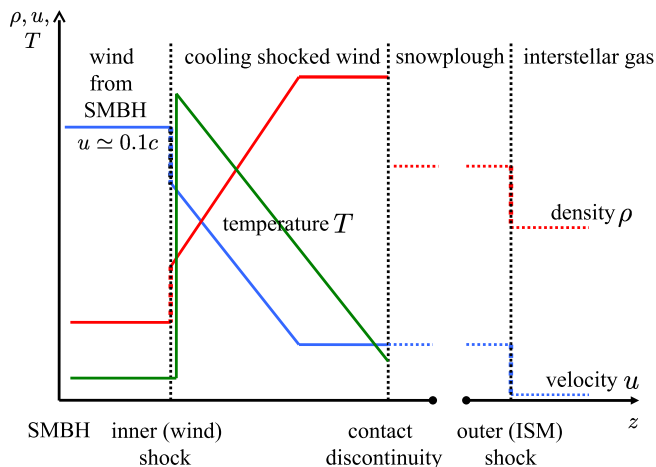


Figure 2. Impact of a wind from an SMBH accreting at a super-Eddington rate on the interstellar gas of the host galaxy: schematic view of the radial dependence of the gas density ρ , velocity u and temperature T . At the inner shock, the gas temperature rises strongly, while the wind density and velocity respectively increase (decrease) by factors ~ 4 . Immediately outside this (adiabatic) shock, the strong Compton cooling effect of the quasar radiation severely reduces the temperature, and slows and compresses the wind gas still further. This cooling region is very narrow compared with the shock radius (see Fig. 1), and may be observable through the and inverse Compton continuum and lower-excitation emission lines. The shocked wind sweeps up the host ISM as a ‘snowplough’. This is much more extended than the cooling region (cf Fig.1), and itself drives an outer shock into the ambient ISM of the host. Linestyles: red, solid: wind gas density ρ ; red, dotted: ISM gas density ρ ; blue, solid, wind gas velocity u ; blue, dotted, ISM gas velocity u ; green, solid, wind gas temperature T . The vertical dashed lines denote the three discontinuities, inner shock, contact discontinuity and outer shock.

$$\frac{l_i u}{\xi} = \text{constant} \quad (15)$$

in this region. We thus expect a correlation between velocity and excitation. The rapid cooling in this region implies a rapid transition between the immediate postshock regime ($\sim v/4$, keV excitation) and the much slower and cooler compressed state. There is direct observational evidence for

this cooling shock in NGC 4051 (Pounds et al., in prep). Pounds et al (2004) had already noted a correlation of outflow velocity with ionization in this source.

5 DYNAMICS

Given the basic structure sketched in the last Section, we can investigate how the shock pattern moves through the interstellar medium of the host galaxy. The cooled postshock gas exerts the ram pressure (14) on the undisturbed interstellar medium of the galaxy, driving an outer shock into it and sweeping it up into a relatively dense shell of increasing mass. The equation of motion of the shell in the momentum-driven limit is

$$\frac{d}{dt}[M(R)\dot{R}] + \frac{GM(R)[M + M_{\text{tot}}(R)]}{R^2} = 4\pi\rho v^2 = \frac{L_{\text{Edd}}}{c} \quad (16)$$

where

$$M(R) = 4\pi \int_0^R \rho_{\text{ISM}} r^2 dr \quad (17)$$

is the swept-up interstellar gas mass, M is the black hole mass, $M_{\text{tot}} = M(R)/f_g$ is the total mass within radius R (including any dark matter), and f_g is the gas fraction (note that in eqn (2) of King, 2005 the suffix ‘tot’ was inadvertently missed off the relevant quantity). This equation takes different forms depending on which part of the host galaxy the shell has reached.

5.1 Close to the black hole

Close to the black hole, i.e. within its sphere of influence, of radius

$$R_{\text{inf}} \simeq \frac{GM}{\sigma^2} \simeq 17M_8\sigma_{200}^{-2} \text{ pc}, \quad (18)$$

the black hole dominates the gravitational potential, and there is essentially no dark matter. Then (16) becomes

$$\frac{d}{dt}[M(R)\dot{R}] + \frac{GM(R)M}{R^2} = \frac{L_{\text{Edd}}}{c} \quad (19)$$

Multiplying through by $M(R)\dot{R}/GM$ we find the first integral

$$\frac{[M(R)\dot{R}]^2}{2GM} = \frac{4\pi}{\kappa} \int M(R)dR - \int \frac{M^2(R)}{R^2} dR. \quad (20)$$

This equation shows that for any reasonable distribution of matter $M(R)$, the shell cannot move outwards unless

$$M(R) \lesssim \frac{4\pi R^2}{\kappa} \sim 2 \times 10^{-4} \left(\frac{R}{R_s}\right)^2 M_8 M_\odot, \quad (21)$$

where we have parametrized the radius in units of the Schwarzschild radius R_s of the black hole, with $M_8 = M/10^8 M_\odot$. The physical content of (21) is that the Eddington thrust cannot lift the weight of a more massive shell at the radius R . An equivalent formulation is

$$\tau = \frac{M(R)\kappa}{4\pi R^2} \lesssim 1 \quad (22)$$

i.e. that the maximum shell mass at a given radius has Thomson depth ~ 1 .

We see that even relatively small amounts of gas sufficiently close to the black hole can stall the outflow. However in this case, the gas from the central Eddington wind would accumulate at the stalled shock until its own mass violated the limit (21). The equivalent (22) shows that the inner wind shock would become optically thick to the quasar radiation, causing multiple scattering and enhancing the momentum

deposition. The postshock pressure would begin to exceed P_{ram} by large factors. Unless the black hole had a very low mass, this enhanced pressure would cause the shell to move out again. This argument shows that the shell moves so as to keep the optical depth of the Eddington wind $\lesssim 1$, i.e.

$$\frac{\dot{M}_{\text{out}} t \kappa}{4\pi R^2} \lesssim 1 \quad (23)$$

so that

$$R \gtrsim \left(\frac{\dot{M}_{\text{out}} \kappa}{4\pi}\right)^{1/2} = 5 \times 10^{16} \dot{m}^{1/2} M_8^{1/2} t_{\text{yr}}^{1/2} \text{ cm} \quad (24)$$

and

$$\dot{R} \gtrsim 1250 \dot{m}^{1/2} M_8^{1/2} t_{\text{yr}}^{-1/2} \text{ km s}^{-1} \quad (25)$$

This implies that the shell would reach a radius $\sim 10^3 R_s$ in no more than a year. At this point the swept-up mass (from (21)) could be as large as $200 m_8 M_\odot$, which would imply an emission measure comparable with an AGN broad-line region. The shell would reach $\sim R_{\text{inf}}$ in $\lesssim 3 \times 10^5$ yr, with a velocity $\dot{R} \gtrsim 2 \text{ km s}^{-1}$.

Thus even a shell whose progress is blocked by an unfavourable matter distribution reaches R_{inf} in about 10^5 yr, assuming that the quasar wind continues to drive it. In the opposite extreme, where the mass of the swept-up matter is low, the time to emerge decreases as $t \sim M_g^{1/2}$, and is limited only by the wind-travel time $\sim 10R/c \sim 500$ yr for arbitrarily low M_g .

This mechanism is clearly limited to the inner parts of a galaxy bulge, as a shell driven in this way can typically only reach radii $\lesssim 200$ pc in a Salpeter time, and $\lesssim 2$ kpc even after a Hubble time. Accordingly we do not consider this mechanism in the next subsection, which treats outflows at radii $> R_{\text{inf}}$.

5.2 Far from the black hole

Far from the black hole (i.e. for $R > R_{\text{inf}}$) the dark matter term M_{tot} becomes dominant in the equation of motion (16), and we can drop the black hole mass term involving M . The condition that the shell should just be able to escape to infinity specifies a relation between the black hole mass M and the parameters of the galaxy potential, particularly the velocity dispersion, i.e. an $M - \sigma$ relation. For a general mass distribution $M_{\text{tot}}(R)$ we can use the first integral (20) to do this. However for a simple isothermal potential the equation of motion has the analytic solution

$$R_{\text{shock}}^2 = \left[\frac{GL_{\text{Edd}}}{2f_g \sigma^2 c} - 2(1 - f_g)\sigma^2 \right] t^2 + 2R_0 v_0 t + R_0^2 \quad (26)$$

where R_0, v_0 are the position and speed of the shell at time $t = 0$ (King, 2005). For large times the first term dominates, and the shell can reach arbitrarily large radii if and only if the black hole mass exceeds the critical value

$$M_\sigma = \frac{f_g(1 - f_g)\kappa}{\pi G^2} \sigma^4 \simeq \frac{f_g \kappa}{\pi G^2} \sigma^4. \quad (27)$$

This is very close to the observed $M - \sigma$ relation (4) (cf King, 2005). At sufficiently large radii the quasar radiation field is too dilute to cool the wind shock, and the shell accelerates beyond the escape value, cutting off the galaxy and establishing the black-hole mass – bulge-mass relation (cf King,

2003, 2005). We see that the time for a continuously-driven shell to reach a given radius $R = 10R_{10}$ kpc is

$$t \simeq \frac{R}{\sqrt{2\sigma(M/M_\sigma - 1)}} \simeq 3.5 \times 10^7 \frac{R_{10}}{\sigma_{200}(M/M_\sigma - 1)} \text{ yr.} \quad (28)$$

For large R_{10} this time is significantly longer than the Salpeter time, implying that the black hole mass M must increase above the threshold value M_σ before the shell reaches large radii. This may suggest that for galaxies with large bulge radii, the black hole mass may tend to lie above the $M - \sigma$ relation. There is some suggestion of this in the observational data (Marconi & Hunt, 2003). However the uncertainty here is in knowing just what radius the shell must reach in order to shut off further accretion on to the black hole.

6 ENERGY-DRIVEN OUTFLOWS

We see from the reasoning of the last Section that the interaction between the quasar wind and its host establishing the $M - \sigma$ relation is – crucially – ‘momentum-driven’ rather than ‘energy-driven’. This equivalent to requiring efficient shock cooling. An energy-driven shock (e.g. Silk & Rees, 1998) would result in a much smaller black hole mass for for a given σ than observed. Instead of the momentum rate L_{Edd}/c balancing the weight of swept-up gas $4f_g\sigma^4/G$, which is what produces the momentum-driven relation (27), an energy-driven shock would equate the energy deposition rate to the rate of working against this weight. In the near-Eddington regime the result is

$$\frac{1}{2}\dot{M}_{\text{out}}v^2 \simeq \frac{\eta}{2}L_{\text{Edd}} = 2\frac{f_g\sigma^4}{G}.\sigma \quad (29)$$

i.e.

$$M(\text{energy}) \simeq \frac{2f_g\kappa}{\eta\pi G^2c}\sigma^5 = \frac{2\sigma}{\eta c}M_\sigma = 3 \times 10^6 M_\odot \sigma_{200}^5, \quad (30)$$

which lies well below the observed relation (4). The coupling adopted in cosmological simulations evidently ensure that the interstellar medium feels the outflow momentum rather than its energy, in addition to the ‘energy efficiency’ $\sim \eta/2 \simeq 0.05$ noted above.

I note finally that if instead of the near-Eddington regime considered here, an energy-driven outflow had a large Eddington ratio $\dot{m} \gg 1$, we would have to replace (29) by

$$\frac{1}{2}\dot{M}_{\text{out}}v^2 \simeq L_{\text{Edd}} = 2\frac{f_g\sigma^4}{G}.\sigma \quad (31)$$

and thus (30) by

$$M(\text{energy}, \dot{m} \gg 1) = \frac{\sigma}{c}M_\sigma = 1.5 \times 10^5 M_\odot \sigma_{200}^5, \quad (32)$$

which is still smaller. Indeed one could imagine a situation in which the central black holes of medium or large galaxies obeyed (32) rather than the observed (4) and self-consistently had central accretion rates well above Eddington, since (6) would now become

$$\dot{m} < \frac{\dot{M}_{\text{dyn}}}{\dot{M}_{\text{Edd}}} \simeq \frac{4.4 \times 10^4}{\sigma_{200}} \simeq \frac{5.2 \times 10^4}{M_\sigma^{1/4}}. \quad (33)$$

The high optical depth implied by the large Eddington ratio might then prevent efficient Compton cooling, justifying the original hypothesis of energy-driven outflow.

It is interesting that observation does not seem to give examples of this possibility, i.e. medium or large galaxies with very low-mass central black holes which could accrete at very high Eddington ratios. The reason may be the inherent tendency of this low-mass sequence to move irreversibly over time to the high-mass case specified by the usual $M - \sigma$ relation (4): thus steady sub- or near-Eddington accretion on to such a hole could eventually increase its mass to the point that it was unlikely to accrete at high Eddington ratios. This would then imply efficient cooling of the shock and thus a momentum-driven outflow.

7 GALAXY-WIDE HIGH-VELOCITY OUTFLOWS

On large scales the outflows described in Section 5.2 above all have (outer) shock velocities limited by the bulge velocity dispersion σ . Yet optical and UV observations give clear evidence of outflows with velocities of several times this value. These cannot be the central quasar winds with $v \sim 0.1c$ discussed in Section 3. Outflows confined within a few parsecs of the black hole may be the near-zone winds inside R_{inf} discussed in Section 5.1, but high-velocity outflows are often seen or inferred on scales comparable with the entire galaxy.

Some of these outflows are seen in compact radio sources (e.g. Holt et al., 2008), some in Seyfert galaxies which are clearly sub-Eddington, and others in post-starburst galaxies (cf Tremonti et al., 2007). The latter could result from the combined effects of stellar winds and supernovae, but the known association of starbursts and AGN leave open the possibility that black holes may be the ultimate driver.

7.1 Outflows from minor accretion events

There is a simple interpretation of such large-scale high-velocity outflows. Consider a galaxy in which the SMBH has reached the mass M_σ given by eqn (27), with the cosmic gas fraction $f_g \simeq 0.16$. Its bulge gas will probably be severely depleted. In a subsequent minor accretion event triggering AGN activity, the effective gas fraction in the bulge will be $f'_g < f_g$. If accretion on to the SMBH becomes super-Eddington for a time $\gtrsim 10^5$ yr, the AGN must drive an outflow shock beyond the radius R_{inf} . However because of the discrepancy between f_g (establishing the black hole mass), and f'_g (the current gas fraction), the shell radius now obeys a modified form of the analytic solution (26), namely

$$R_{\text{shock}}^2 = \left[\frac{GL_{\text{Edd}}}{2f'_g\sigma^2c} - 2(1 - f'_g)\sigma^2 \right] t^2 + 2R_0v_0t + R_0^2 \quad (34)$$

where the L_{Edd} term involves f_g rather than f'_g . Thus at large t we have

$$R_{\text{shock}}^2 = 2 \left[\frac{f_g}{f'_g}(1 - f_g) - (1 - f'_g) \right] \sigma^2 t^2 \simeq 2\frac{f_g}{f'_g}\sigma^2 t^2 \quad (35)$$

where we have taken $f'_g \ll f_g < 1$ in the last form. This shows that the shell reaches velocities

$$\simeq (2f_g/f'_g)^{1/2}\sigma > \sigma, \quad (36)$$

because its inertia is much lower than the one previously expelled by the Eddington thrust in the accretion episode which defined the SMBH mass. If at some point the AGN activity turns off, we can match another solution of the form (26), but with L_{Edd} formally = 0, to the solution (34). This solution reveals that a coasting shell stalls only at distances $\sim (f_g/f'_g)^{1/2}$ times its radius R_0 at the point when AGN activity ceased, and thus persists for a timescale $R_0/\sigma \sim 10^8$ yr, (cf 28).

Episodic minor accretion events of this type therefore naturally produce large-scale outflows with velocities $> \sigma$. Moreover, since they persist as fossil winds long after the AGN has become faint, they can have total momentum considerably higher than could be driven by the *current* AGN radiation pressure, i.e. well in excess of the apparent momentum limit.

7.2 Outflows from major accretion events

There is a second possible type of rapid outflow on large spatial scales. It is inherently rarer than those triggered by minor accretion events, as described in the previous subsection, but represents a decisive stage in the evolution of the galaxy.

Consider a major Eddington accretion event in which the central SMBH attains its critical mass M_σ . Equation (27) shows that the resulting momentum-driven outflow does not stall, as it does for lower SMBH masses, but continues out to large radii. Beyond a critical radius, the quasar radiation field is too dilute to cool the wind shock on its (momentum-driven) flow time t_{flow} . If Eddington accretion on to the central SMBH is still continuing, the outflow becomes energy-driven. The extra thermal energy now accelerates the shell further, eventually to a terminal speed

$$v_e \simeq \left[\frac{2\eta\sigma^2 c}{3} \right]^{1/3} \simeq 875\sigma_{200}^{2/3} \text{ km s}^{-1} \quad (37)$$

(King, 2005). This is fast enough to drive gas out of the galaxy potential entirely.

This process ultimately limits the gas content of the galaxy bulge and hence establishes the black hole–bulge mass relation (King, 2003, 2005). It is clearly a rarer type of event than outflows driven by minor accretion events as described above. A clear observational distinction is that these rare energy-driven outflows require that the quasar driving the outflow should be radiating at the Eddington limit.

8 CONCLUSION

We have shown that Eddington accretion episodes in AGN produce winds with velocities $v \sim 0.1c$ and ionization parameters $\xi \sim 10^4$ (cgs) requiring the presence of resonance lines of helium- and hydrogenlike iron. These properties follow from momentum and mass conservation, and agree with recent X-ray observations of high-speed outflows from AGN. Because the winds have speeds $\sim 0.1c$ they can persist long after the AGN have become sub-Eddington.

The wind creates a strong cooling shock as it impacts the interstellar medium of the host galaxy. This cooling region may be observable, as it produces an inverse Compton

continuum and lower-excitation emission lines associated with lower velocities. The shell of matter swept up by the (‘momentum-driven’) shocked wind emerges from the black hole’s sphere of influence on a timescale $\lesssim 3 \times 10^5$ yr. The shell then stalls unless the black hole mass has reached the value M_σ implied by the $M-\sigma$ relation. If the wind shock did not cool, as suggested here, the resulting (‘energy-driven’) outflow would imply a far smaller SMBH mass than actually observed. In galaxies with large bulges the black hole must grow somewhat beyond this value, suggesting that the observed $M-\sigma$ relation may curve upwards at large M . Galaxy-wide outflows with velocities significantly exceeding σ probably result from minor accretion episodes with low gas fractions. These can appear as fossil outflows in galaxies where there is little current AGN activity. In rare cases it may be possible to observe the energy-driven outflows which sweep gas out of the galaxy and establish the black hole–bulge mass relation. However these require the quasar to be at the Eddington luminosity.

9 ACKNOWLEDGMENTS

I thank Ken Pounds and Sergei Nayakshin for illuminating discussions. Theoretical astrophysics research at Leicester is supported by an STFC rolling grant.

REFERENCES

- Abramowicz M. A., 2009, ASPC, 403, 29
 Begelman M. C., King A. R., Pringle J. E., 2006, MNRAS, 370, 399
 Cappi M., 2006, AN, 327, 1012
 Chartas G., Brandt W. N., Gallagher S. C., 2003, ApJ, 595, 85
 Denney K. D., et al., 2009, ApJ, 702, 1353
 Di Matteo T., Springel V., Hernquist L., 2005, Natur, 433, 604
 Ferrarese L., Merritt D., 2000, ApJ, 539, L9
 Gebhardt K., et al., 2000, ApJ, 539, L13
 Häring N., Rix H.-W., 2004, ApJ, 604, L89
 Holt J., Tadhunter C. N., Morganti R., 2008, MNRAS, 387, 639
 King A., 2003, ApJ, 596, L27
 King A., 2005, ApJ, 635, L121
 King A., 2009, ApJ, 695, L107
 King A. R., Taam R. E., Begelman M. C., 2000, ApJ, 530, L25
 King A. R., Pounds K. A., 2003, MNRAS, 345, 657
 Krongold Y., Nicastro F., Elvis M., Brickhouse N., Binette L., Mathur S., Jiménez-Bailón E., 2007, ApJ, 659, 1022
 Lodato G., King A. R., Pringle J. E., 2009, MNRAS, 392, 332
 Marconi A., Hunt L. K., 2003, ApJ, 589, L21
 O’Brien P. T., Reeves J. N., Simpson C., Ward M. J., 2005, MNRAS, 360, L25
 Pounds K. A., Reeves J. N., King A. R., Page K. L., O’Brien P. T., Turner M. J. L., 2003a, MNRAS, 345, 705
 Pounds K. A., King A. R., Page K. L., O’Brien P. T., 2003b, MNRAS, 346, 1025
 Pounds K. A., Reeves J. N., King A. R., Page K. L., 2004, MNRAS, 350, 10
 Pounds K. A., Reeves J. N., 2009, MNRAS, 397, 249
 Silk J., Rees M. J., 1998, A&A, 331, L1
 Shakura N. I., Sunyaev R. A., 1973, A&A, 24, 337
 Soltan A., 1982, MNRAS, 200, 115
 Tremonti C. A., Moustakas J., Diamond-Stanic A. M., 2007, ApJ, 663, L77
 Yu Q., Tremaine S., 2002, MNRAS, 335, 965